Effect of the spreading solvent on the three-phase contact angle of microparticles attached at fluid interfaces

A. Maestro, L. J. Bonales, H. Ritacco, R. G. Rubio and F. Ortega*

Received 14th May 2010, Accepted 28th July 2010
DOI: 10.1039/c0cp00570c

We address a systematic study of the three-phase contact angle, θ, of microparticles at flat fluid–liquid interfaces by using different experimental methods. We measured the dependence of θ not only on the particle chemical composition and size, but also on the solvent used to spread the microparticles onto the fluid interface. We found a non-expected and non-regular dependence of θ with size, chemical nature and spreading solvent used for the different particles studied. We propose that these dependences are due to porosity/roughness of the particles that allows the adsorption of the spreading solvent onto the solid particle surface. This conclusion is supported by the values of the line tensions estimated for the different systems.

Introduction

Colloidal particles can accumulate onto the interface dividing two immiscible fluid phases and stabilize foams and emulsions by slowing down the three processes that lead to the phase separation: drainage, coarsening and coalescence. This fact was discovered at the beginning of the last century by Ramsden[1] and rediscovered by Pickering[2,3] some years later but then forgotten until the appearance of the work of Menon and coworkers on water–oil emulsions in 1987.[4] Since those early works the interest on dispersed systems stabilized by particles has greatly increased due to new ways for producing nano or micro structured materials, and the range of applications of such particles. For instance, Dinsmore *et al.*[5] reported a novel method to fabricate permeable solid capsules by assembling particles at the surface of an aqueous drop in a continuous oil phase. These capsule, called *Colloidosomes*, allow one to encapsulate a wide range of active molecules, which may be delivered in a controlled way. Particles at fluid interfaces are also important from the environmental point of view (*e.g.* by reducing the use of standard surfactants) in water treatment and recycling flotation process.[6] Recently, particles attached to fluid interfaces or in confined environments (membranes, cells) have been used as probes to measure the surface shear viscoelasticity of those systems by following their Brownian motion. This methodology leads to a new rheological technique called micro- or nano-rheology, depending of the size of the particles, with several advantages over traditional methods.[7]

The behaviour of particles at interfaces (structure, interaction forces and dynamics) is also important because they can be used as a model system to study 2D or quasi-2D colloidal organization. The structure and dynamics of these systems has been studied mainly at flat fluid–fluid interfaces (air/oil–water) such as Langmuir films.[8–10] To prepare Langmuir monolayers of particles, they are deposited onto an interface using a spreading solvent, usually an alcohol. The basic knowledge of particles at flat liquid interfaces was reviewed by Aveyard *et al.*[11] and Binks *et al.*[12,13] The traditional method to characterize these particle monolayers are based in the study of the surface pressure–area (Π–A) isotherms.[14–17] For microparticles, these monolayers can be also characterized by video-microscopy obtaining information about their structure and dynamical behaviour.[18] The forces between particles at the monolayer have been studied by using laser tweezers, and also different theoretical models of the pair interaction potential have been proposed.[12,19–21]

The wettability of the particles has been found to be a key factor in controlling the static and dynamic behavior of particle at the fluid interfaces. This wettability is characterized by the three-phase contact angle θ which is defined as the angle between the tangents to the solid surface and the interface measured through one of the phases. When the lower subphase is water, particles with angles between $0^\circ < \theta < 90^\circ$ are called hydrophilic, because the particle area immersed into the water phase is larger than the area in contact with the upper phase. On the contrary, particles are called hydrophobic when $90^\circ < \theta < 180^\circ$. Nowadays, it is well known that the contact angle θ determines the type of foam or emulsion formed; for instance, *foams* or *water-in-oil emulsions* are formed if $\theta < 90^\circ$ while *aerosols* or *oil-in-water emulsions* are formed when $\theta > 90^\circ$. The wettability of the particles remarkable affects the free energy of particle detachment, ΔG_d, and thus the particle capability to stabilize foams and emulsions. Pieranski[22] has calculated the detachment free energy for the case of a planar fluid interface as a function of the three-phase contact angle,

$$\Delta G_d = \pi a^2 \gamma_0 (1 - |\cos\theta|)^2 \quad (1)$$

where a is the particle radius and γ_0 the surface tension. This equation yields a maximum in the free energy of particle detachment at $\theta = 90^\circ$, where ΔG_d is several orders of magnitude greater than the thermal energy $k_B T$, (k_B being the Boltzmann constant), and sufficient to make the particle attachment almost irreversible. On the other hand, ΔG_d decreases to zero at $\theta = 0^\circ$ and $\theta = 180^\circ$ and particles can exhibit a reversible attachment-detachment behaviour.

Grupo de Sistemas Complejos, Departamento de Química Física I, Facultad de Química, Universidad Complutense, 28040-Madrid, Spain. E-mail: fortega@quim.ucm.es

Different authors have demonstrated that the particle wettability has a dramatic effect on the particle interactions resulting in ordered or disordered structures or aggregation depending on the θ.[12] For instance, Kralchevsky *et al.*[23] have shown that very hydrophobic silica particles adsorbed at the octane–water interface, with $\theta \approx 130^\circ$, lead to well-ordered monolayers over large distances, while less hydrophobic particles ($\theta \approx 118^\circ$) form large aggregates. Lin and Chen found a 2D solid-like phase, which melts through a hexatic phase for charged polystyrene particles adsorbed at decane–water interface with $\theta \approx 70^\circ$.[24,25] Fernandez-Toledano *et al.* have proposed a theoretical model of interactions between particles in monolayers and they have calculated the total pair potential by computing the different interaction terms.[26] The computation of their potential has been done using the Derjaguin approximation over the emergent and immersed parts of the particles which depends on the three phase contact angle. These authors obtained a dependence of the repulsive dipolar interaction potential on θ for different inter-particle distances with a maximum near 90° in all cases. However the strength of the dipolar interaction decreases several orders of magnitude for θ below 20° and above 120°.[26]

Particles can be used as probes to measure the surface shear viscosity of Langmuir monolayers made of different materials in micro- and nano-rheology experiments. To extract useful information from these experiments one needs to understand the physics underlying the motion of the particles in a 2D or quasi-2D environment. Here, the contact angle plays a key role in calculating the interfacial shear viscosity from the Brownian trajectories of the particles, as described by Danov *et al.* and Fischer *et al.*[27–29] These authors have calculated the drag force on a small spherical particle attached to interfaces with different viscosities as a function of the contact angle.

The contact angle, measured trough the lower subphase, is given in its simplest way by the Young's equation, and depends only on the interfacial tensions between the upper (air or oil) and lower (water) phases (γ_0) and the ones between the solid particle and both upper (γ_{po}) and lower phases (γ_{pw}),

$$\cos\theta = \frac{\gamma_{po} - \gamma_{pw}}{\gamma_0} \qquad (2)$$

In the last decades increasing number of publications have appeared describing different methods to measure the contact angle θ for microparticles at interfaces.[30] They can be classified in two families: "*in situ*" methods, based on the direct observation of the particle at the interface[14] and those in which the forces involved in the adsorption are measured.[30,31] In contrast to other particle properties, like charge or size, this parameter is hardly accessible experimentally. The direct determination of θ is restricted to particles of sufficiently large size because of the magnification limits. Thus, direct optical microscopy methods are suitable for particle diameters of several tens of micrometres. The determination of θ from a force–distance dependence measured by AFM is also limited by the size of a particle glued to the tip of the cantilever. For further discussion about the direct and indirect methods see ref. 30.

Here we present a systematic study of the contact angle of microparticles adsorbed onto flat liquid–liquid and liquid–gas interfaces as a function of the particle chemical nature and size. We explore for the first time, the influence of the spreading solvent on the measured contact angle and found that the chemical nature of the used solvent strongly modifies the measured angles. We have used three different methodologies to measure θ. Concretely, we have used the gel-trapping technique developed by Paunov,[32,33] the method based on the measurement of collapse pressure in a particulate monolayer upon compression in the Langmuir trough[31] and the method based on the excluded-area formalism.[30] It will be shown that the three methods lead to comparable values of θ.

Experimental

Chemicals

Microparticles of different chemical nature and sizes were used in the experiments. (a) Negatively charged surfactant-free polystyrene (PS) microparticles with sulfate functional groups on the surface (Interfacial Dynamics Corporation, USA), with diameters ranging from 0.5 to 5.7 μm. All of them have similar surface charge density (≈ -6 μC cm^{-2}). (b) Poly(methyl methacrylate) (PMMA) microparticles (Microparticles GmbH, Germany) with two diameters, 1.0 and 2.0 μm. The first ones are electrostatically stabilized by sulfate groups on their surface and the second ones are sterically stabilized by PVAc (polyvinyl acetate) adsorbed on the surface. (c) Silica-sphere particles (SiO_2) with OH groups at their surface and 1.0 μm in diameter (Sigma-Aldrich, Germany). Water with a resistivity higher than 14 MΩ obtained from a milli-Q (Millipore) was used and n-octane (Sigma-Aldrich) filtrated trough an alumina (Al_2O_3) column was used as the oil-subphase. The spreading solvents used were: 2-propanol (IPA) (99%) and methanol (MetOH) (99%), used as received from Sigma-Aldrich (Germany).

Methods

We have used the gel trapping technique (GTT) to measure the three-phase contact angle of different sets of PS, silica and PMMA particles spread onto air–water and octane/water interfaces by using MetOH and IPA as spreading solvents.[33] In this technique a non surface active gelling agent (Gellan) is added to the water, the particles are spread onto the interface at about 50 °C, and after gelling the water phase by cooling the system at room temperature (25 °C), the particle monolayer is detached by using polydimethylsiloxane (PDMS), which is first poured on top of the water and then cured. The surface of PDMS with the trapped particles is imaged with a Scanning Electron Microscope (SEM). The position of the particles with respect to the PDMS surface can be then determined from the SEM images, which provides the necessary information for the determination of the particle contact angle at the initial air–water or oil–water interface. Fig. 1 shows a typical SEM image. We have chosen this technique because it can be also used to observe the behaviour of all different types of solid particles (nature and size) at both liquid interfaces.[33] We have also used the method described by Clint and Taylor[31] in which θ is obtained from the Π–A isotherms of the particle monolayers. The surface pressure is defined as usual, $\Pi = \gamma_0 - \gamma$,

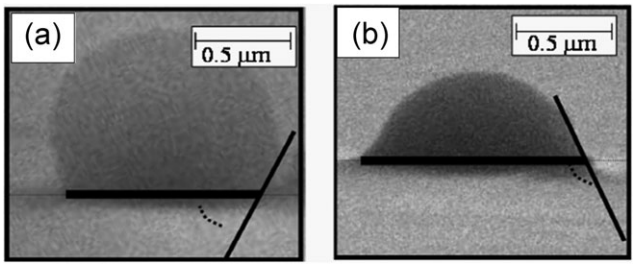

Fig. 1 Set of SEM images of SiO_2 particles with 1.0 μm in diameter spread onto the octane–water interface with (a) isopropanol and (b) methanol obtained by the GTT. Straight lines show the contact line of the particle at the PDMS surface which allows one to calculate θ.

being γ_0 and γ the surface tension of a bare interface and with the monolayer, respectively, and A is the interfacial area. The contact angle is related to the collapse pressure, $\Pi_{collapse}$ (see Fig. 2) through:

$$\cos\theta = \pm\sqrt{\frac{\Pi_{collapse}2\sqrt{3}}{\pi\gamma_0}} - 1, \qquad (3)$$

where $2\sqrt{3}$ is a geometry constant that comes from the hexagonal packing of the particles at the collapse. Hence by measuring the interfacial tension and collapse pressure we obtain the contact angle. We could only use this method for monolayers that pack in solid hexagonal arrays on compressing the monolayer as happens in the oil–water interface using IPA as spreading solvent.

The third method is based on the excluded-area formalism.[30] Monolayers composed of a mixture of an insoluble polymer and the microparticles are considered as a binary surfactant monolayer with complete immiscibility of its components. The area occupied by the particles at the interface is then inaccessible for the polymer chains, and therefore, the Π–A isotherms for the mixed monolayer should show a shift towards higher molecular areas, A, when increasing the number of particles, N_p. From the slope of the excluded area

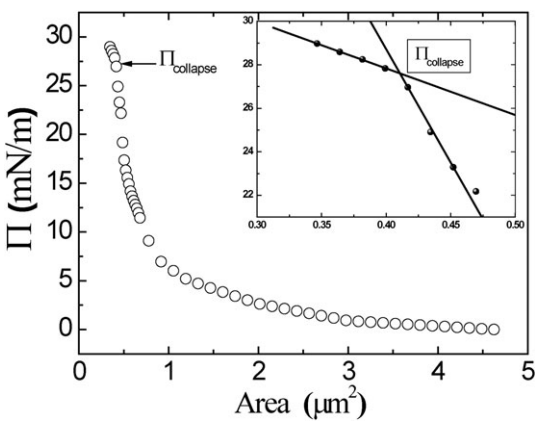

Fig. 2 Surface preasure–area isotherm for 0.5 μm PS particles at octane–water interface. The inset shows the collapse presure, $\Pi_{collapse}$, obtained by the locus of the slope change. The surface pressure due to the spreading solvent is neglected because the small amount injected in comparison with the total volume of water.

as a function of surface pressure, the averaged interfacial area occupied by the particles and θ can be calculated as:

$$\frac{d\Delta A}{d\Pi} = -\frac{2N_p\pi a^2\gamma_0^2\cos^2\theta_p^0}{\gamma^3} \qquad (4)$$

being $\theta_p{}^0$ the contact angle measured against the liquid phase in the initial uncovered state.

Results and discussion

Let us first report the different methodologies to determinate θ used in this work. Fig. 1 shows a set of images obtained by SEM of PMMA particles trapped in PDMS using the GTT corresponding to identical particles spread with methanol (Fig. 1a) and with isopropanol (Fig. 1b) onto the octane–water interface. One can clearly observe that the contact angles depend on the spreading solvent. This change in the contact angle θ could be due to the different surface activity of the alcohols that will change γ_0 according to Young's equation. To test this possibility, we have performed control experiments by spreading the same amounts of methanol and isopropanol that are added when spreading the particles. The surface tension measured at both interfaces (air/octane–water) did not change with the added amount of alcohols (volume spread is less than 0.1%), which means that the change in the contact angle cannot be attributed to the adsorption of the alcohols onto the interface. Table 1 summarizes all the contact angle measured by the GTT of particles with different chemical nature (PS, PMMA, and SiO_2) attached to the air–water and oil–water interface as a function of their diameter σ, and for two different spreading solvents (methanol and isopropanol).

Fig. 2 shows as example a surface pressure-area (Π–A) isotherm of a monolayer of PS particles (σ = 0.548 mm) at the octane–water interface. At large areas the surface pressure is very low, when the area is reduced particles begin to interact and the surface pressure increases until a kink which corresponds to the collapse pressure ($\Pi_{collapse}$) of the monolayer. We have calculated the $\Pi_{collapse}$ as the inflection point, where a slope change occurs (inset in Fig. 2). From $\Pi_{collapse}$ and using eqn (3) we obtained two solutions θ = 77.6° and 102.4°.

Table 1 Three-phase contact angle of microparticles of different nature attached to air/oil–water interfaces using two different spreading solvent, *i.e.*, methanol (MetOH) and isopropanol (IPA), obtained by GTT. Values between parenthesis correspond to the excluded area methodology, and the one with (*) to the method proposed by Clint and Taylor (ref. 31)

		Water–air		Octane–water	
	Diameter/μm	MetOH	IPA	MetOH	IPA
PS	**0.5**	—	—	—	74 ± 5 77.6 ± 0.9*
	1.0	63 ± 7	121 ± 10	28 ± 7	140 ± 10
	1.6	89 ± 8	88 ± 9	56 ± 6	120 ± 12
	2.9	76 ± 6	59 ± 2	120 ± 11	135 ± 10
	5.7	37 ± 2	30 ± 8	119 ± 13	120 ± 9
PMMA	**1.0**	18 ± 6 (15 ± 3)	36 ± 6 (31 ± 3)	—	—
	2.0	29 ± 4 (26 ± 2)	56 ± 2 (56 ± 1)	—	—
SiO_2	**1.0**	41 ± 10	70 ± 10	68 ± 6	148 ± 5

As can be seen in the Table 1 the first value is in agreement with the contact angle obtained by the GTT.

Fig. 3 is an example of the third methodology used to obtain the contact angle based on the excluded-area formalism. It shows the surface pressure-area isotherms Π–A of a monolayer formed by a mixture of a polymer, poly(methyl methacrylate) (PMMA, Molecular weight M_w = 270.8 kDa) and *ca.* 12×10^6 and 20×10^6 particles of PMMA (diameter σ = 2 μm), respectively. Similar shifts were obtained for other particle concentrations and for the rest of the PMMA particles. The inset in Fig. 3 shows the excluded area by the PMMA particles; *i.e.*, the difference between the area of the monolayer with PMMA particles attached and the area of the monolayer only formed by the polymer. From the slope of the excluded area *versus* surface pressure, the averaged interfacial area occupied by the particles can be calculated, and from it the contact angle θ of the particles at the interface (eqn (4)). For instance, for the PMMA particles (σ = 2 μm) both slopes in Fig. 3, (A/Π corresponding to $N = 12 \times 10^6$ and 20×10^6 particles, lead to a mean value of $\theta = 56 \pm 1°$, which is in excellent agreement with the value obtained by GTT, $\theta_{GTT} = 56 \pm 2°$. All values obtained with this method agree within 5–10% with the results from the GTT.

The values of θ shown in Fig. 4 denote the existence of a non-general behavior in the relation of θ with the spreading solvent, hereinafter '*solvent effect*'. The behavior of the contact angle *vs.* particle size and spreading solvent change cannot be explained by the Young relation (eqn (1)) because it does not take into account the particle size. Furthermore, eqn (1) is only valid when particles are completely smooth and adsorbed at the interface without spreading solvent (Gibbs monolayers) as will be demonstrated in the next paragraph. It is well known that real solid surfaces are usually rough and chemically heterogeneous, especially for polymeric/gel particles, which

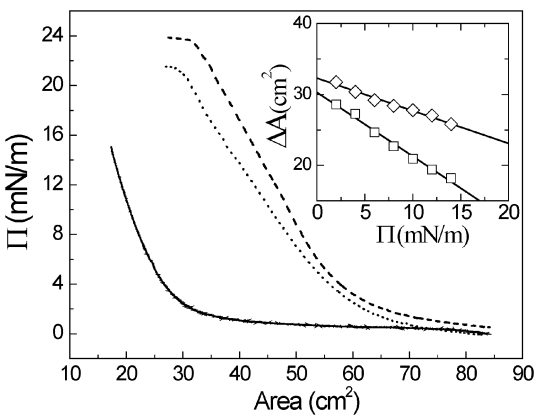

Fig. 3 Surface pressure–area isotherms Π–A measured for monolayers of poly(methyl methacrylate) (PMMA) Langmuir films. Solid line represent the bare PMMA monolayer, dotted line and dashed line represent the PMMA monolayer with 12×10^6 and 20×10^6 particles of PMMA with a diameter σ = 2 μm respectively. The inset shows the excluded area, *i.e.*, the difference between the area of the monolayer with PMMA particles attached and the area of the monolayer only formed by the polymer as a function of the surface pressure Π. The solid line represent the linear fit of the experimental data. The slope of the fit $\Delta A/\Pi$ is related to the contact angle of the PMMA particles.

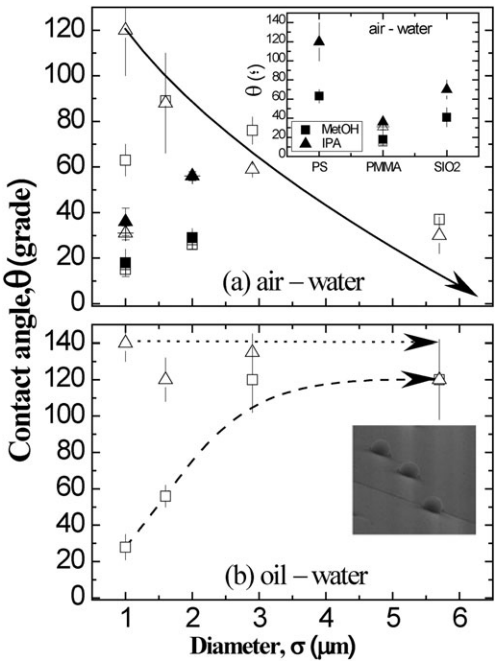

Fig. 4 Three-phase contact angle θ as a function of the diameter σ of the particles attached to the interface (a) air–water and (b) oil–water. The nature of the particles and the spreading solvent as follows: Polystyrene (PS) particles spread with methanol (□), and isopropanol (△). Poly(methyl methacrylate) (PMMA) particles in methanol (■), (⊞) and isopropanol (▲), (⟑) using GTT and the excluded area formalism, respectively. In (a) the general θ–σ dependency is denoted by a solid line and in (b) the θ–σ behaviour for MetOH and IPA is denoted by a dashed and dotted line, respectively. Upper inset: Contact angle as a function of the chemical nature of the particles attached at the air–water interface.

show porosity and high surface roughness.[24,34] It should be emphasized that the roughness and/or the existence of a heterogeneous surface lead to two important effects. The first one is that roughness magnifies the line tension (τ) effect. Three phases in contact meet at a line and then there exist a *line tension* which is expressed as a force or energy per unit length. Line tension can be viewed as the equivalent to the surface tension (energy per unit area for a 2D interface dividing two phases) and it should be considered that for spherical microparticles the effect of τ becomes more important as the radius decreases. In the limit of ideal flat surface $\tau \to 0$ and the original Young equation is recovered. The relevant modification of the Young equation reads:[35]

$$\cos\theta = \cos\theta_{Young} - \frac{\tau}{a_c \gamma_0} \qquad (5)$$

where θ_{Young} is the three-phase contact angle from the Young relation, a_c is the radius of the contact line between the three phases and τ is the line tension.[36,37] Taking into account the roughness of the particles, the second effect mentioned above is related to traces of solvent that could be trapped at the particle surface in the spreading process. Therefore, the surface tensions related by the Young equation (eqn (2)) and then the three-phase contact angle, are affected by the trapped solvent as sketched in Scheme 1. In addition, this adsorption will also change the length of the contact line.

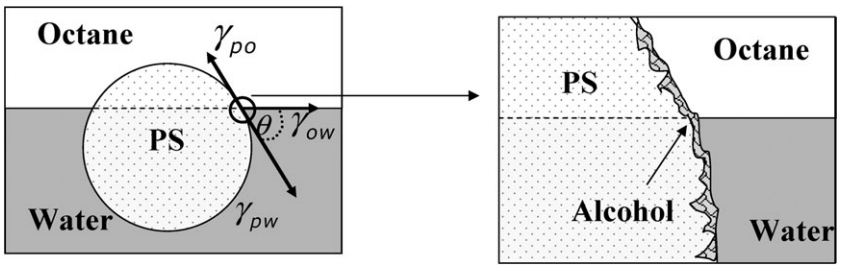

Scheme 1 Detail of the spreading solvent trapped on the roughness of the particle's surface for an arbitrary oil–water interface.

Fig. 4 shows the experimental contact angle θ of particles whose surfaces have different chemical nature (PS, PMMA and SiO_2) attached to the air–water interface (Fig. 4a) and octane–water interface (Fig. 4b) as a function of their diameter σ, taking into account the different spreading solvent used. We found a general tendency for the values of θ corresponding to PS particles at the air–water interface (spread with both IPA and MetOH); *i.e.*, θ decreases as the diameter of the particle increases which is pointed out by the solid line (Fig. 4a). Particles with different nature (PS, PMMA and SiO_2) spread with IPA lead to higher contact angles than using MetOH, (see inset in Fig. 4). Fig. 4(b) shows the experimental θs obtained for PS particles at the oil–water interface. Here, two different behaviors were found: the contact angle θ increases (PS spread from MetOH) or remain constant (from IPA) as the diameter increases. The opposite occurs at W/A interface, as previously described. Thus, we propose that particles spread with IPA are at this interface completely covered with the alcohol molecules leading to a constant contact angle as a function of the particle diameter. To test our hypothesis we have measured the contact angle of PS particles with equal size (2.9 μm), and different charge surface density, (−5.7 and −9.7 μC cm^{-2}), similar contact angle values were obtained. A possible explanation of this behaviour is that particles are completely covered by a layer of the spreading solvent and, as a consequence, the nature of the surface does not affect the contact angle.

In particular, PS particles with size ranging from 1.0 to 1.6 μm behave as a completely hydrophilic ($\theta < 90°$) when are spread from MetOH, and are hydrophobic ($\theta > 90°$) when IPA is used as the spreading solvent. IPA is less hydrophilic than MetOH, thus, the contact angle of particles spread with IPA lead to higher contact angles than the same particles spread with MetOH.

In general, the *solvent effect* seems to be more important for small particles. This fact could be due to an increase of roughness and porosity as diameter particles decreases. However, when the particle size increase we suppose that the solvent does not cover the surface completely, thus leading to similar contact angle for particles spread from different solvents. Unfortunately there are no available experimental data showing the dependence of roughness/porosity on the particle size.

In addition, we estimate the value of the line tension for our systems using eqn (4). In Fig. 5 we have plotted cos θ as a function of $(a \sin(\theta))^{-1}$ for PS particles spread with both solvents at the octane–water interface and also at the air–water interface as shown in the inset of Fig. 5. We have consider smooth particles where $a_c = a \sin\theta$. Considering $\gamma_0 = 72$ mN m^{-1}

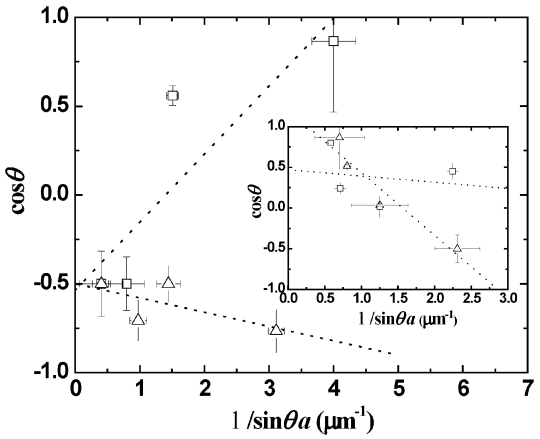

Fig. 5 cos θ as a function of $1/ac$ (where $ac = \sin\theta\,\sigma/2$) PS particles with different diameter (σ) at the oil–water interface. Symbols as follows: Particles spread with methanol (□) and isopropanol (△). The dotted line represents the best fit of the experimental data by eqn (5). The slope of the fit is related to the line tension τ. Inset: Similar results at the air–water interface.

for the air–water interface we found $\tau \approx 0.5$ nN and $\tau \approx 5$ nN from the slope for, respectively, methanol and IPA. The line tension is much higher for IPA than for methanol which is a further indication of an interaction between the spreading solvent and the solid particles. For the octane–water interface ($\gamma_0 = 51$ mN m^{-1}) and PS particles, we found a negative line tension, $\tau \approx -0.20$ nN for methanol and a positive one with IPA, ($\tau \approx 0.20$ nN), being again a clear indication of a preferential adsorption of the spreading solvent onto the surface of the particles. This is also supported by the values of the ordinate *y*-intercept of the fitting lines in Fig. 5, which gives us an estimation of the $\cos(\theta_{Young})$. For the water–octane interfaces these values are negative indicating that the difference between the particle–octane interfacial tension (γ_{po}) minus the particle–water one (γ_{pw}) is negative, *i.e.* $\gamma_{po} < \gamma_{pw}$ which is consistent with the presence of methanol or isopropanol adsorbed onto the solid surface (the surface tension between methanol or isopropanol and octane is lower than between them and water).

Conclusions

This study reveals the non-regular behaviour of the contact angle of particles adsorbed at fluid interfaces with the chemical nature and size of the particles and with the spreading solvent. We have used three different methods to measure the contact

angle (explained in the main text) which leads to similar results. We demonstrate how the contact angle θ depends strongly on many commented factors not taken into consideration previously. Our results point out that the roughness and/or porosity of particles play a key role in the hydrophobicity/hydrophilicity balance of the particles accounting by θ. We highlight the existence of a solvent effect: molecules of solvent can be trapped at the particle surface in the spreading process changing quantitatively the contact angle. This conclusion is supported by the values of the line tensions estimated for the different systems

Acknowledgements

This work was supported in part by MCINN under grant FIS2009-14008-C02-01, by ESA under grant MAP A0-00-052 and by EU under ITN-Multiflow. A. M. and L. J. B. were supported by a FPU and FPI fellowships from MICINN. H. R. acknowledges financial support from a RyC contract of MICINN. L. J. B. thanks V. N. Paunov for provide the gellan used in the GTT and helping us with this technique. This work greatly benefits from the discussions with D. Langevin and R. Hidalgo. The authors are grateful to the CAI de Microscopia of the University Complutense for the use of the SEM facility.

References

1 W. Ramsden, *Proc. R. Soc. London*, 1903, **72**, 156–164.
2 S. U. Pickering, *J. Chem. Soc.*, 1907, **97**.
3 E. Lucassen-Reynders and M. van den Tempel, *J. Phys. Chem.*, 1963, **67**.
4 V. B. Menon, R. Nagarajan and D. T. Wasan, *Sep. Sci. Technol.*, 1987, **22**, 2295–2322.
5 A. D. Dinsmore, M. F. Hsu, M. G. Nikolaides, M. Marquez, A. R. Bausch and D. A. Weitz, *Science*, 2002, **298**, 1006–1009.
6 A. V. Nguyen and H. J. Schulze, *Colloidal Science of Flotation*, Marcel Dekker, New York, 2003.
7 F. Ortega, H. Ritacco and R. Rubio, *Curr. Opin. Colloid Interface Sci.*, 2010, **15**(4), 237–245.
8 H. Schuker, *Kolloid-Z*, 1967, **380**, 216.
9 E. Sheppard and N. Tcheurekdjian, *J. Colloid Interface Sci.*, 1968, **28**, 481.
10 A. Doroszkowski, *J. Poymer Sci.*, 1971, **34**, 253.
11 R. Aveyard, B. P. Binks and J. H. Clint, *Adv. Colloid Interface Sci.*, 2003, **100–102**, 503–546.
12 B. P. Binks, *Colloidal Particles at Liquid Interfaces*, UK, 2006.
13 B. P. Binks, *Curr. Opin. Colloid Interface Sci.*, 2002, **7**, 21.
14 R. Averyard, J.-H. Clint and V. N. Paunov, *Langmuir*, 2000, **16**, 1996.
15 R. Averyard, J.-H. Clint, D. Nees and N. Quirke, *Langmuir*, 2000, **16**, 8820.
16 T. S. Horozov, R. Averyard, B. P. Binks and J. H. Clint, *Langmuir*, 2005, **21**, 7405–7412.
17 Z. Hórvölgyi, S. Nëmath and J. H. Fendle, *Langmuir*, 1996, **12**, 997–1004.
18 T. M. Fischer, P. Dhar and P. Heinig, *J. Fluid Mech.*, 2006, **558**, 451.
19 P. Pieranski, *Phys. Rev. Lett.*, 1980, **45**, 569.
20 R. Aveyard, B. P. Binks, J. H. Clint, P. D. I. Fletcher, T. S. Horozov, B. Neumann and V. N. Paunov, *Phys. Rev. Lett.*, 2002, **88**, 246102.
21 F. Martínez-López, M. A. Cabrerizo-Vílchez and R. Hidalgo-Alvarez, *J. Colloid Interface Sci.*, 2000, **232**, 303.
22 P. Pieranski, *Phys. Rev. Lett.*, 1980, **45**, 569–572.
23 P. A. Kralchevsky, V. N. Paunov, I. B. Ivanov and K. Nagayama, *J. Colloid Interface Sci.*, 1992, **151**, 79–94.
24 W. Chen, S. S. Tan, T. K. Ng, W. T. Ford and P. Tong, *Phys. Rev. Lett.*, 2005, **95**.
25 B. J. Lin and L. J. Chen, *Colloids Surf., A*, 2006, **284–285**, 239–245.
26 J. C. Fernandez-Toledano, A. Moncho-Jorda, F. Martinez-Lopez and R. Hidalgo-Alvarez, *Langmuir*, 2006, **22**, 6746–6749.
27 T. M. Fischer, P. Dhar and P. Heinig, *J. Fluid Mech.*, 2006, **558**, 451–475.
28 J. T. Petkov, N. D. Denkov, K. D. Danov, O. D. Velev, R. Aust and F. Durst, *J. Colloid Interface Sci.*, 1995, **172**, 147–154.
29 K. D. Danov, R. Dimova and B. Pouligny, *Phys. Fluids*, 2000, **12**, 2711–2722.
30 D. O. Grigoriev, J. Kragel, V. Dutschk, R. Miller and H. Möhwald, *Phys. Chem. Chem. Phys.*, 2007, **9**, 6447–6454.
31 J. H. Clint and S. E. Taylor, *Colloids Surf.*, 1992, **65**, 61.
32 R. Aveyard, J. H. Clint, D. Nees and V. N. Paunov, *Langmuir*, 2000, **16**, 1969–1979.
33 V. N. Paunov, *Langmuir*, 2003, **19**, 7970–7976.
34 S. S. Tan, R. L. Sherman, D. Q. Qin and W. T. Ford, *Langmuir*, 2005, **21**, 43–49.
35 R. J. Good and M. N. Koo, *J. Colloid Interface Sci.*, 1979, **71**, 283–292.
36 G. Wolansky and A. Marmur, *Langmuir*, 1998, **14**, 5292–5297.
37 A. Marmur and B. Krasovitski, *Langmuir*, 2002, **18**, 8919–8923.

